Morphological disparity in the skull of Amazon River dolphins of the genus *Inia* (Cetacea, Iniidae) is inconsistent with a single taxon

Renata Emin-Lima,[1] Fabio A. Machado,[2] Salvatore Siciliano,[3] Waleska Gravena,[4] Enzo Aliaga-Rossel,[5] José de Sousa e Silva, Junior,[1] Erika Hingst-Zaher,[6,*] and Larissa Rosa de Oliveira[7,8]

[1]*Museu Paraense Emílio Goeldi, Coordenação de Zoologia, Setor de Mastozoologia, Grupo de Estudos de Mamíferos Aquáticos da Amazônia (GEMAM), Av. Perimetral, 1901, Terra Firme, Belém, PA 66077-530, Brazil*
[2]*Department of Biology, Virginia Tech, Blacksburg, Virginia 24061, USA*
[3]*Escola Nacional de Saúde Pública/Fiocruz, Depto. de Ciências Biológicas, R. Leopoldo Bulhões, 1480 - Manguinhos, Rio de Janeiro, RJ 21041-210, Brazil*
[4]*Universidade Federal do Amazonas Instituto de Saúde e Biotecnología, Estrada Coari Mamiá, 305, Coari, AM 69460-000, Brazil*
[5]*Universidad Mayor de San Andrés, Instituto de Ecología, Cota Cota Calle 27 n/n, Campus Universitario, La Paz, Bolivia*
[6]*Instituto Butantan, Museu Biológico, Av. Vital Brazil, 1500, São Paulo, SP 05503-900, Brazil*
[7]*Universidade do Vale do Rio dos Sinos, Laboratório de Ecologia de Mamíferos, Av. Unisinos 950, bloco E04, sala E04229, São Leopoldo, RS 93022-000, Brazil*
[8]*Grupo de Estudos de Mamíferos Aquáticos do Rio Grande do Sul (GEMARS), Rua Bento Gonçalves, 165/1002, Torres, RS 95560-000, Brazil*

*To whom correspondence should be addressed: hingstz@gmail.com

The taxonomy of the South American river dolphins of the genus *Inia* has been a focus of intense debate. While traditionally it is thought to be composed of a single species with three geographically structured subspecies (*Inia geoffrensis geoffrensis*, *I. g. humboldtiana*, and *I. g. boliviensis*), recent molecular studies have highlighted substantial differentiation, suggesting the existence of two species (*I. geoffrensis* and *I. araguaiaensis*). Despite this evidence, the recognition of the specific status of these taxa has been hindered by inconsistent morphological diagnoses. Here, we aim to provide evidence for the morphological differentiation (or lack thereof) between subspecies and putative species. We employ geometrics and traditional morphometrics to measure skull variation to support efforts of integrative taxonomy. Our results show that morphometric diversity within the group is inconsistent with a single taxon. Morphometric evidence supports the traditional differentiation of three distinct morphotypes within the analyzed sample. These morphotypes largely correspond to described subspecies *I. g. geoffrensis*, *I. g. humboldtiana*—the latter differing from the former by size—and *I. g. boliviensis*, which differs from the remaining groups by shape. Furthermore, morphometric data show no differences between *I. g. geoffrensis* and a newly proposed species, *I. araguaiaensis*. Given the conservation importance of this genus and the different threats they are subject to, we strongly suggest an urgent integrative taxonomic treatment of the group to better protect these singular cetaceans.

Key words: geometric morphometrics, shape, size, traditional morphometrics

A taxonomia dos golfinhos de água doce da América do Sul pertencentes ao gênero Inia têm sido foco de intenso debate. Enquanto tradicionalmente considera-se a existência de uma única espécie e três subespécies (*Inia geoffrensis geoffrensis*, *I. g. humboldtiana*, and *I. g. boliviensis*), estudos moleculares recentes evidenciam diferenciação substancial, sugerindo a existência de mais de uma espécie (*I. geoffrensis* and *I. araguaiaensis*). Apesar desta evidência, o reconhecimento do status específico desses táxons tem sido limitado pela presença de diagnoses morfológicas inconsistentes. Nosso objetivo no presente trabalho é proporcionar evidências para a diferenciação morfológica (ou a sua ausência) entre as subespécies e as possíveis espécies. Utilizamos

morfometria geométrica e tradicional para medir a variação do cranio de forma a sustentar esforços de taxonomia integrativa. Nossos resultados mostram que a diversidade morfométrica dentro do grupo é inconsistente com um único táxon. A evidência morfométrica aponta a diferenciação tradicional de três morfotipos distintos dentro da amostra analisada. Esses morfotipos correspondem em grande parte às subespecies *I. g. geoffrensis*, *I. g. humboldtiana*, que diverge da primeira através do seu tamanho, e *I. g. boliviensis*, que diverge das demais através de sua forma. Ademais, dados morfométricos não mostram diferenças entre *Inia g. geoffrensis* e a espécie recém proposta, *I. araguaiaensis*. Dada a importância para conservação desse gênero e as diferentes ameaças às quais estão sujeitos, nós sugerimos enfaticamente um tratamento de taxonomia integrativa para o grupo, de forma a melhor proteger esses cetáceos singulares.

Palavras-chave: forma, morfometria geométrica, morfometria tradicional, tamanho

River dolphins are a paraphyletic group composed of four genera of odontocetes: *Lipotes* (Baiji) and *Platanista* (Ganges dolphin), which live in rivers at opposite ends of the Asian continent; and in South America, *Pontoporia* (Franciscana dolphin) and *Inia* (Amazon River dolphin; Hamilton et al. 2001). Because of their habitat requirements (large bodies of freshwater rivers and coastal areas), close proximity to human activities, and poor conservation status (Smith et al. 2017; Silva et al. 2018; Zerbini et al. 2018; Braulik and Smith 2019), understanding their diversity and taxonomy is an extremely pressing issue to inform proper conservation efforts. However, despite the relative advances in systematics and taxonomy of river dolphins in the last decades (e.g., Hamilton et al. 2001; Banguera-Hinestroza et al. 2002; Gravena et al. 2014), the diversity of the group could still be underestimated, robbing potentially vulnerable species of their protected status. Among these species, the taxonomy of the Amazon River dolphins (*Inia*), a group endemic to the Amazon region, has been under intense debate (Hrbek et al. 2014).

Traditionally, the genus *Inia* was thought to be composed of a single species with three subspecies (Rice 1998): *Inia geoffrensis geoffrensis*, *I. g. boliviensis*, and *I. g. humboldtiana*. These subspecies are geographically isolated, inhabiting different river basins of the Northern region of South America (Best and Silva 1989; Aliaga-Rossel 2002; Banguera-Hinestroza et al. 2002; Gravena et al. 2014). Both *I. g. geoffrensis* and *I. g. boliviensis* inhabit the Amazon River basin, with *I. g. geoffrensis* ranging throughout the basin, and with *I. g. boliviensis* restricted to the Beni-Mamoré and Madeira River basins, isolated by the Teotônio rapids in the Madeira River (Aliaga-Rossel 2002; Gravena et al. 2014; Aliaga-Rossel and Duran 2020). *Inia g. humboldtiana* inhabits the Orinoco River basin, isolated from the former two subspecies by the Casiquiare channel (Meade and Koehnken 1991; Banguera-Hinestroza et al. 2002). Molecular studies have corroborated that these taxonomic units represent genetically distinct groups, suggesting that the structure of the river basins can impose severe restrictions to gene flow, leading to population structuring and differentiation (Hollatz et al. 2011; Gravena et al. 2014, 2015; Hrbek et al. 2014). Specifically, population structure associated with potential geographic barriers led to the proposal of a new species from the Tocantins–Araguaia basin, *I. araguaiaensis* (Hrbek et al. 2014). This species is thought to have diverged vicariously

from *I. geoffrensis* about 2 Ma and now is distributed along the Tocantins and Araguaia rivers and in Marajó Bay (Siciliano et al. 2016). Furthermore, the molecular differentiation between *I. g. geoffrensis* and *I. g. boliviensis* is enough to suggest that *I. g. boliviensis* also warrants specific status (Hrbek et al. 2014; Siciliano et al. 2016). However, the acceptance of new species within *Inia* has been problematic due to, in part, the lack of clear phenotypic diagnostics and small number of morphological samples (Society for Marine Mammalogy Committee on Taxonomy 2021).

In the present contribution, we aim to provide new evidence for the morphological differentiation (or lack thereof) between *Inia* subspecies and putative species. To that end, we employed geometrics and traditional morphometrics to measure skull variation to support efforts of integrative taxonomy (e.g., Miranda et al. 2018; Machado and Teta 2020). The use of morphometrics has been employed in taxonomic studies of aquatic mammals (e.g., Monteiro-Filho et al. 2002; Oliveira et al. 2008; Wickert et al. 2016) and has helped to recognize differences between the tucuxi (*Sotalia fluviatilis*) and Guiana dolphin (*S. guianensis*; Monteiro-Filho et al. 2002; Caballero et al. 2007), and to propose a putative species of *Tursiops* (Wickert et al. 2016). Here, we use this approach to evaluate if morphological disparity in *Inia* is consistent with the existence of a single taxon, as currently recognized (Society for Marine Mammalogy Committee on Taxonomy 2021).

Materials and Methods

Samples.—All adult *Inia* skulls available in the following scientific collections were analyzed: *Museu Paraense Emílio Goeldi* (MPEG), *Museu de Zoologia da Universidade de São Paulo* (MZUSP), *Museu Nacional, Universidade Federal do Rio de Janeiro* (MN), *Pontifícia Universidade Católica de Minas Gerais* (PUC-MG), *Universidade Federal do Tocantins* (UFT), *American Museum of Natural History* (AMNH), and *The National Museum of Natural History* (USNM). Only adults were selected and examined to avoid variability due to growth. Specimens were identified as such when the basioccipital–basisphenoid suture was totally fused and closed, according to Silva (1994). This procedure resulted in a sample of 46 specimens, 38 of which were used in the geometric morphometric analysis and 46 were used in the traditional morphometric analysis (Table 1; Appendix I).

Table 1.—Sample size analyzed in geometric and traditional morphometrics analyses. IA: *Inia araguaiaensis*; IB: *Inia boliviensis*; IG: *Inia geoffrensis*; IH: *Inia humboldtiana*.

Sex		Female	Male	Unknown	Total
Geometric morphometrics	IA	2	2	5	9
	IB	2	2	0	4
	IG	8	5	7	20
	IH	0	4	1	5
	Total	12	13	13	38
Traditional morphometrics	IA	1	3	10	14
	IB	2	2	3	7
	IG	7	8	5	20
	IH	0	4	1	5
	Total	10	17	19	46

To evaluate if we could pool individuals from both sexes in the same analysis, we tested for the presence of sexual dimorphism on various linear measurements for *I. g. geoffrensis*, which presented the largest sample with known sex (Table 1). For each measurement, we performed a *t*-test to assess statistical significance of differences between sexes. Additionally, we evaluated differences in size and shape using univariate and multivariate nonparametric linear models for the same group (see below).

Specimens were assigned a priori to groups based on the river system of origin and named based on their hypothetical species status (each species was considered an operational taxonomic units; OTUs) for statistical hypothesis testing (Fig. 1).

Individuals from the Araguaia–Tocantins River system were assigned to IA (*Inia araguaiaensis*), from the Beni-Mamoré River basin to IB (*I. boliviensis*), from the Amazon River basin to IG (*I. geoffrensis*), and from the Orinoco River basin to IH (*I. humboldtiana*).

Size and shape variation.—Twenty-nine anatomical landmarks were digitized on the skulls (Fig. 2) with a *3D MicroScribe* digitizer to create models suitable for statistical analysis of three-dimensional shape. Landmark definitions was adapted from Monteiro-Filho et al. (2002), Galatius (2010), and Sydney et al. (2012). Missing landmarks were estimated using a Thin Plate Spline (TPS) interpolation technique, which deforms one target configuration into the specimen containing missing data (Adams et al. 2020). Missing data interpolation was done in two steps. First, if a configuration lacked landmarks on only one side of the skull, we performed the TPS interpolation of that specimen on a mirror image of itself. Secondly, if the same landmark was missing from both sides or was along the midline, we performed the TPS interpolation using the average configuration of the geographically nearest four specimens as a target. The resulting configurations were subjected to a generalized Procrustes analysis (Rohlf and Slice 1990) and projected into a tangent Euclidean space for statistical analysis (Slice 2001). The Procrustes residuals of this analysis (the difference between the coordinates of the average shape and each superimposed configuration) were used as shape variables. Size was calculated as the centroid size (CS; square-root of the sum of squared distances between the configuration center of gravity and each landmark) of the configuration. For data visualization and
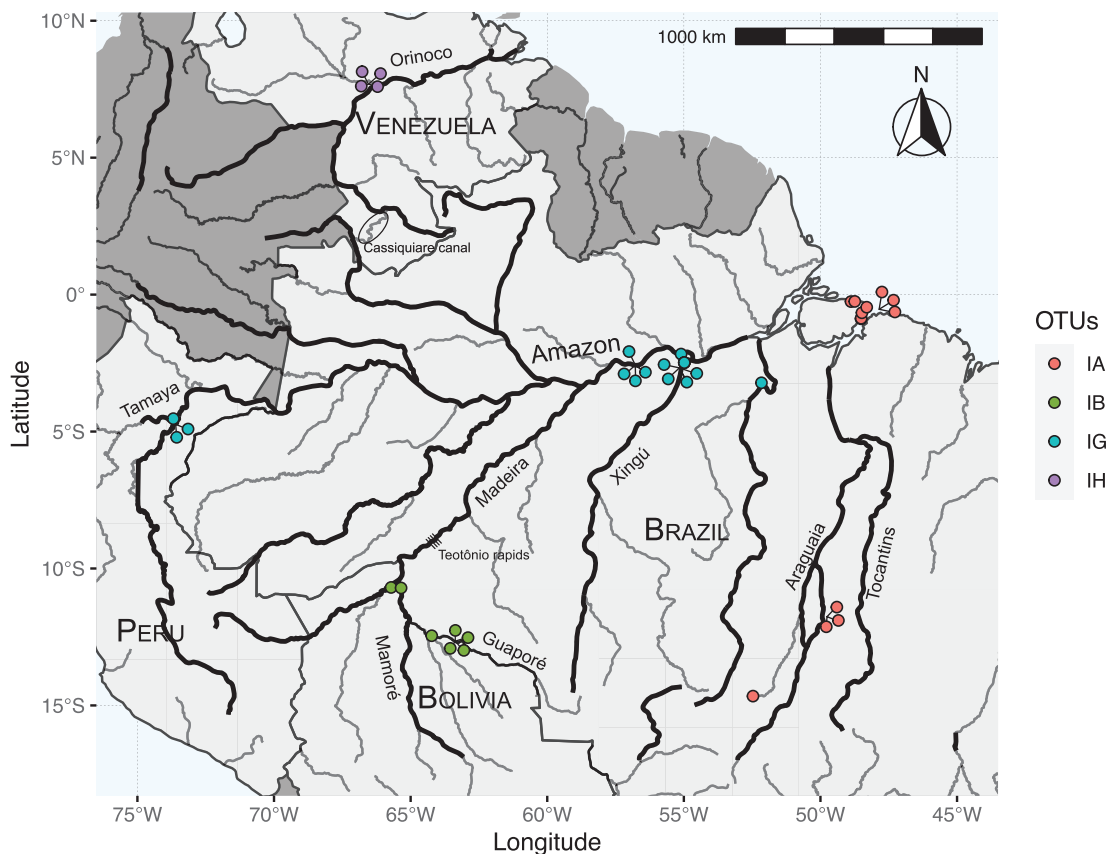
Fig. 1.—Geographic distribution of samples included in the present analysis.
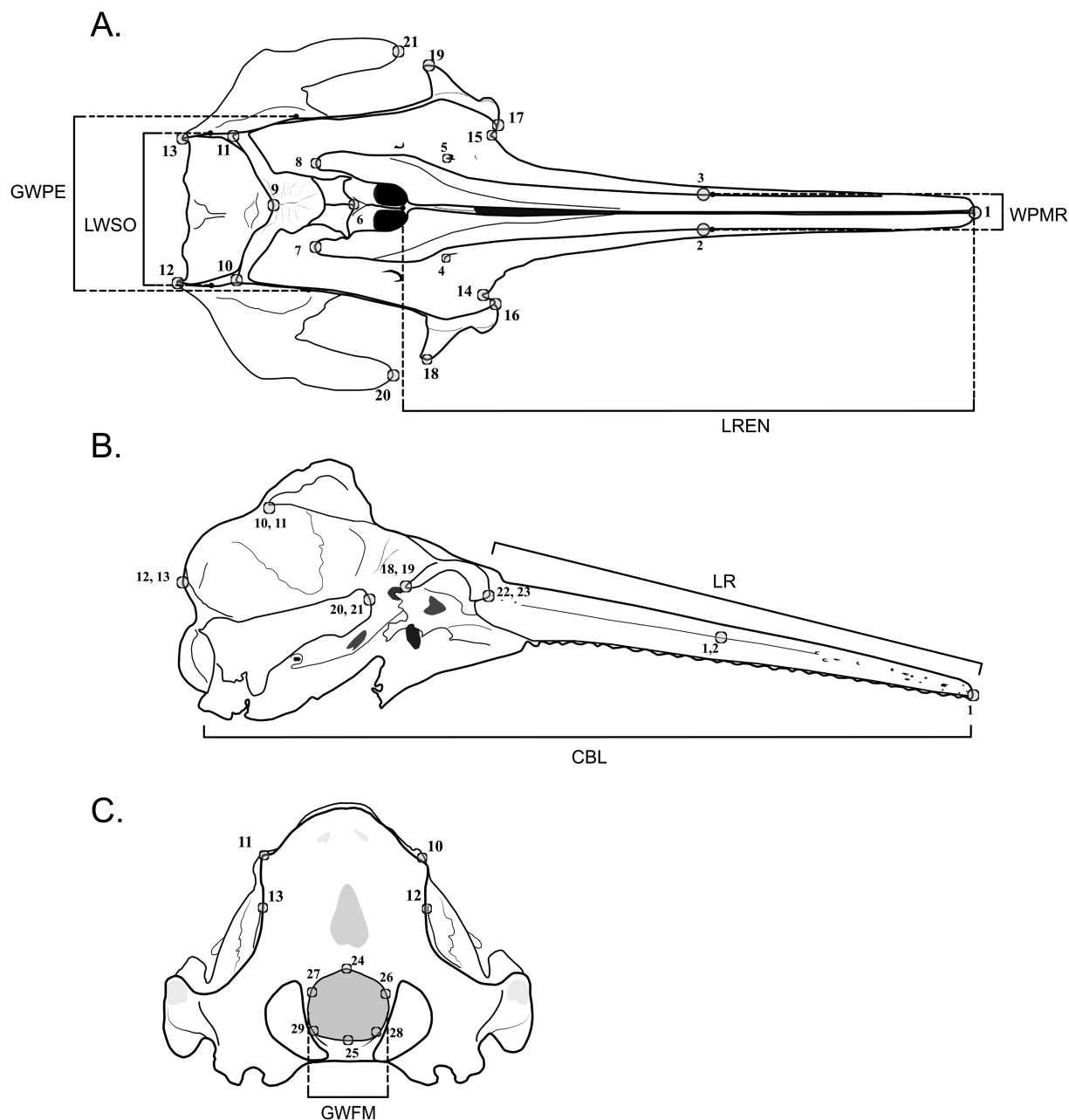
Fig. 2.—Three-dimensional landmarks (numbers) and linear measurements (acronyms) for (A) dorsal, (B) lateral, and (C) occipital views of the skull of *Inia geoffrensis* (MN06425). Bilateral landmarks are displayed on the same point on the lateral view, separated by a comma. Description of landmarks and measurements can be found in Appendix II. Here we only display measurements mentioned in the main text for simplicity. Illustration courtesy of Maira Laeta.

dimensionality reduction, we computed a principal component analysis (PCA) on both Procrustes residuals and the logarithm of the centroid size (logCS). The resulting morphospace, the "size–shape" or form space, contains information about both size and shape variation (Mitteroecker et al. 2004; Klingenberg 2016).

To test for differences among sexes within *I. g. geoffrensis*, we performed a nonparametric analysis of variance (np-ANOVA) for logCS and nonparametric multivariate analysis of variance (np-MANOVA) for shape (Anderson 2001; Collyer and Adams 2018). To investigate size differences between groups, we performed a np-ANOVA on logCS. To identify which groups differ from each other in terms of size, we performed a pairwise

Wilcoxon rank-sum test, adjusting the significance for multiple tests using the Holm method. Finally, to test for shape differences among species groups, we performed a nonparametric multivariate analysis of covariance (np-MANCOVA) on shape. We introduced logCS as a covariate to investigate if shape differences were due to differences in allometric scaling alone (Monteiro-Filho et al. 2002; Sydney et al. 2012). Effects sizes and the null distribution for nonparametric methods were obtained using randomization of residuals in a permutation procedure (Collyer and Adams 2018), using 9,999 permutations.

Since the np-MANCOVA only evaluates group differences globally, we conducted a canonical variate analysis (CVA)

using the OTUs as factors to inspect pairwise group differences. Given that size was an important factor influencing shape change between groups (see Results), we conducted a size-free CVA. Specifically, we calculated the residual shape variation after controlling for a common allometric component (or CAC) for all groups (Mitteroecker et al. 2004), which excludes the allometric shape variation from the sample. Because CVA is sensitive to high variable-to-specimen ratios (Strauss 2010; Mitteroecker and Bookstein 2011), we used the five leading axes of a PCA on the residual shape variation as input to the CVA. To evaluate pairwise group differences, we calculated between-group Mahalanobis distances for the allometry-free shape space. The significance of each group difference was assessed by shuffling group identities 1,000 times and recalculating the distances.

Traditional morphometrics.—To provide a more intuitive approach to discern between OTUs, we also investigated the skull morphological variation in *Inia* using traditional morphometrics. We obtained 21 caliper measurements from 46 skulls (Fig. 2; Appendix II). Measurements were modified from those taken previously for *I. geoffrensis* (Pilleri and Gihr 1977; Casinos and Ocaña 1979; Silva 1994) and other cetaceans (Perrin 1975) and were measured using digital calipers. Morphometric variables were taken as a ratio between the measured value and the condylobasal length of the skull (CBL) to account for size differences.

To examine differences among OTUs, we conducted a series of univariate ANOVAs for CBL and each shape ratio. Variables deemed significantly different among OTUs were further investigated using pairwise *t*-tests. Significance (*P*-values) for both ANOVAs and pairwise *t*-tests were corrected for multiple tests using the Holm method.

Teeth count.—Differences in teeth count were evaluated for maxillary (TnS) and mandibular teeth count (TnI). The number of teeth alveoli were counted on both left and right sides of the skull. Because differences between sides were small (usually differing in only one tooth), we averaged the teeth count of both sides, producing a single value for each individual. Differences between OTUs were tested globally using a nonparametric Kruskal–Wallis rank-sum test for both TnS and TnI. If differences were found, a pairwise Wilcoxon rank-sum test was used to identify which group differed from the others. The significance for multiple tests was corrected using the Holm method. All statistical analyses were performed using R (R Core Team 2021).

Results

Sexual dimorphism.—None of the *t*-tests performed on the cranial measurements of IG produced significant results with and without correction for multiple tests (*P*-values = 1 or >0.055, respectively). The same was true for the investigation of logCS (d.f. = 1, SS = 0.011, MS = 0.011, R^2 = 0.189, F = 2.567, Z = 1.029, *P*-value = 0.160; statistical terminology as in Table 2) and Procrustes residuals (d.f. = 1, SS = 0.003, MS = 0.003, R^2 = 0.094, F = 1.144, Z = 0.466, *P*-value = 0.312).

Table 2.—Nonparametric analysis of variance (ANOVA) to test differences in size between operational taxonomic units (OTUs) (A) and nonparametric multivariate analysis of covariance (MANCOVA) of shape data evaluating the influence of size and OTU membership, and their interaction on the shape variation (B). d.f.: degrees of freedom; SS: sum of squares; MS: mean squares; R^2: coefficient of determination; F: Fisher F-statistics; Z: Z-transformed effect size; *P*-value: probability of observed effect size Z under an empirically generated null distribution. Significant values (α = 0.05) are marked in bold.

	d.f.	SS	MS	R^2	F	Z	*P*-value
A. Size							
OTU	3	0.107	0.036	0.368	6.411	2.789	**0.003**
Residuals	33	0.183	0.006	0.632			
Total	36	0.290					
B. Shape							
Size	1	0.009	0.009	0.060	2.807	2.831	**0.005**
OTU	3	0.038	0.013	0.257	4.038	3.868	**0.001**
Size:OTU	3	0.008	0.003	0.052	0.822	-0.618	0.722
Residuals	29	0.090	0.003	0.615			
Total	36	0.146					

Therefore, we pooled males, females, and individuals with unknown sex assignment to improve sample sizes in all downstream analyses.

Size and shape variation.—The first two leading axes of the PCA of the size and shape data showed some discrimination between the a priori defined OTUs (Fig. 3). PC1 explained ~70% of the total variation and depicts a contrast between small individuals with negative scores and large individuals with positive scores. The main group differentiation along this axis was related to the IH OTU, which was considerably smaller on average than other groups. PC2 explained ~10% of the total variation and depicts a contrast between a robust morphotype on negative scores and a more gracile morphology with a slightly elongated rostrum and smaller braincase on the positive scores of this axis. The main group discrimination along this axis refers to the discrimination of IB with positive scores from the remaining OTUs.

The nonparametric ANOVA on logCS showed that OTUs differ in size (Table 2). Specifically, the pairwise Wilcoxon rank-sum test showed that the primary differentiation is between IH from both IA and IG (Fig. 4). The nonparametric MANCOVA revealed that shape was significantly affected by size (Table 2), even though it explained a small portion of the shape differentiation (R^2 = 0.065; Z = 3.284). This implies that allometry plays a role, albeit small, in the shape differentiation of these OTUs. The differentiation between groups was also significant and accounted for a large portion of the variation in our sample, even after accounting for size variation (R^2 = 0.274; Z = 4.186). The interaction between size and OTU membership was not considered significant in our analyses, suggesting that all groups possess a similar size–shape relationship. These results indicate that OTUs diverge from each other on size, allometric, and nonallometric shape components.

The CVA on the allometry-free shape data showed the differentiation of IB on the leading axis, with great overlap between groups on the second axis (Fig. 5). Differentiation along CV1 is similar to shape differences depicted by PC2
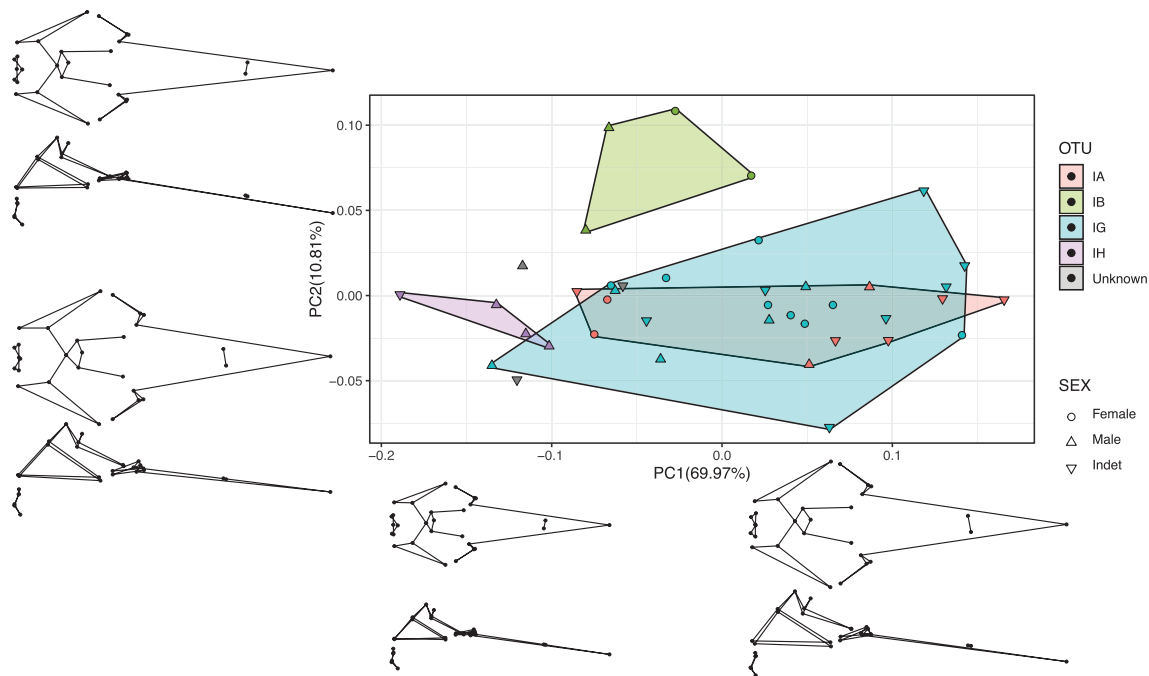
Fig. 3.—The first two leading principal components of the size–shape data (Procrustes residuals + log-centroid size) of *Inia*. Polygons are convex hulls encapsulating all observations of the same operational taxonomic unit (OTU). Wireframes depict morphological differences between extreme values of each principal component. IA: *Inia araguaiaensis*; IB: *Inia boliviensis*; IG: *Inia geoffrensis*; and IH: *Inia humboldtiana.* Gray shapes indicate specimens with unknown taxonomic affinity.
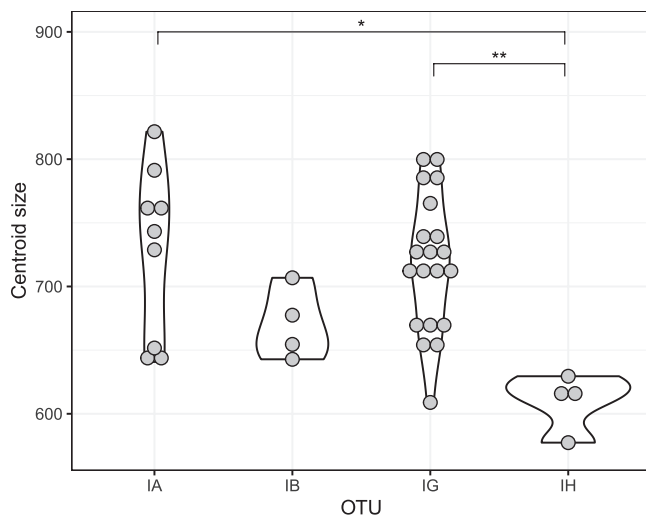
Fig. 4.—Distribution of centroid size of the skull among *Inia* operational taxonomic units (OTUs). Asterisks represent the significance level of the Wilcoxon rank-sum tests corrected for multiple comparisons (*$P < 0.05$; **$P < 0.01$). IA: *Inia araguaiaensis*; IB: *Inia boliviensis*; IG: *Inia geoffrensis*; and IH: *Inia humboldtiana*.

(Fig. 3), while differences in CV2 are mostly restricted to the asymmetry of the nasal opening region (higher values are more asymmetric) and the relative size of the squamosal (higher values associated with squamosal being more anteriorly displaced). Some IA showed higher values on the CV2, falling outside the range observed for other taxa. The Mahalanobis distance permutation analyses corroborated these findings, with IB being significantly different from the remaining OTUs (Table 3).

Linear measurements.—After correction for multiple comparisons, only condylobasal length (CBL), and the shape ratios of the length of rostrum (RL), width of premaxillae at midlength of rostrum (WPMR), greatest width of preorbital (GWPE), least width of supraorbital (LWSO), and greatest width of the foramen magnum (GWFM) were considered significant in the ANOVAs ($P < 0.03$). However, when investigated with the pairwise *t*-tests, only WPMR and LWSO showed significant differences between OTUs (Fig. 6A). Specifically, IB showed significantly smaller values for these ratios than both IA and IG, but not from IH. Furthermore, IH showed a significantly smaller WPMR than IA, but did not differ from IB and IG for this variable, nor did it differ from any other group on LWSO.

Teeth count.—Teeth counts were considered significantly different between OTUs for both maxillary (TnS-χ^2 = 25.215, d.f. = 3, *P*-value = 1.392e-05) and mandibular teeth (TnI-χ^2 = 23.76, d.f. = 3, *P*-value = 2.804e-05). The pairwise Wilcoxon rank-sum tests showed that IB differs from the remaining OTUs by having higher TnS and TnI counts (Fig. 6B). IH was significantly different from IB and IG for having lower mandibular and maxillary teeth counts, while IA did not differ from either IG or IH on any count.

DISCUSSION

Molecular studies of the genus *Inia* have repeatedly shown marked between-group differentiation and reproductive isolation, even leading to the proposal of new taxa (Hamilton et al. 2001; Banguera-Hinestroza et al. 2002; Hollatz et al. 2011; Gravena et al. 2014; Hrbek et al. 2014; Siciliano et al. 2016). However, the scarcity of morphological studies and,
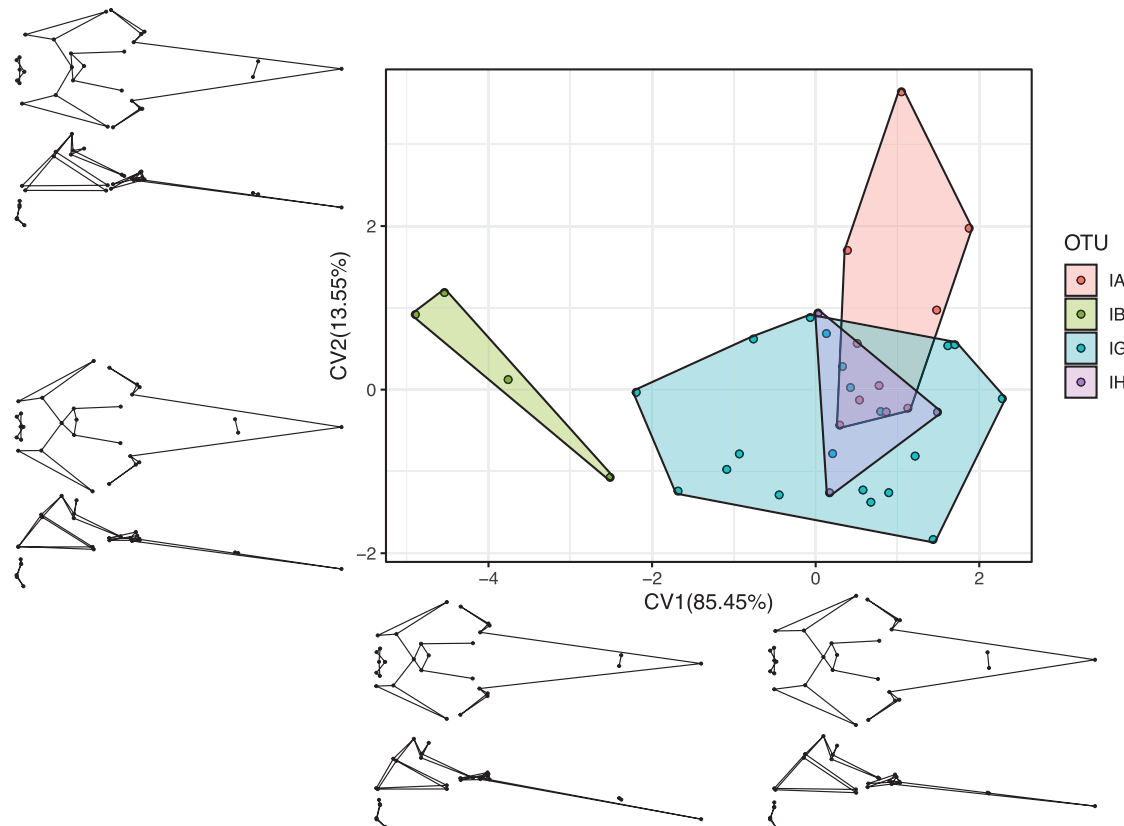
Fig. 5.—The first two leading axes of canonical variate analyses for allometry-free shape data. Morphological variation along CV1 is similar to variation depicted along PC2 (Fig. 2). Polygons are convex hulls encapsulating all observations of the same operational taxonomic unit (OTU). IA: *Inia araguaiaensis*; IB: *Inia boliviensis*; IG: *Inia geoffrensis*; and IH: *Inia humboldtiana*.

Table 3.—Mahalanobis permutation analysis for between-group differentiation. Values below the diagonal refer to the Mahalanobis distance and above diagonal values are *P*-values. Significant values (α = 0.05) are marked in bold. IA: *Inia araguaiaensis*; IB: *Inia boliviensis*; IG: *Inia geoffrensis*; IH: *Inia humboldtiana*.

|	IA	IB	IG	IH
IA		**0.001**	0.076	0.696
IB	5.591		**0.001**	**0.001**
IG	1.563	4.834		0.961
IH	2.940	4.632	2.316	

consequently, of diagnostic features have slowed down the acceptance of these new taxa (Society for Marine Mammalogy Committee on Taxonomy 2021). Our results show that the morphometric diversity within the group supports the existence of three distinct morphotypes instead of a single one. These morphotypes largely correspond to described subspecies *I. g. geoffrensis*, *I. g. boliviensis*, and *I. g. humboldtiana*.

In our sample, specimens assigned to the taxa *I. araguaiaensis* and *I. g. geoffrensis* showed a more robust skull morphology, while *I. g. humboldtiana* and *I. g. boliviensis* have a more gracile skull (Figs. 3, 4, and 6A). In the case of *I. g. humboldtiana*, the taxon could have achieved this morphology by reducing skull size in relation to the more robust taxa (i.e., allometry; Figs. 3 and 4; Table 2). Considering that we only analyzed adults, it is possible that *I. g. humboldtiana* is a paedomorphic taxon, a phenomenon

not necessarily uncommon for Odontoceti (Fettuccia et al. 2009; Galatius 2010; Loy et al. 2011; Sydney et al. 2012). In the case of *I. g. boliviensis*, however, morphological changes did not align with allometric trends of variation (Figs. 3 and 5; Table 2), with individuals from this population presenting a skull of similar size to those of the robust morphotype while showing relatively smaller braincase and a narrower and longer rostrum (Figs. 3 and 6A). In addition to these differences, *I. g. boliviensis* also showed more teeth than any other group (31–35 teeth in lower tooth row and 29–33 upper tooth row; Fig. 6B). Considering that allometry is a common mammalian constraint to evolution, the presence of morphological differences that do not fall along a size gradient is a strong indicator of between-species differentiation (e.g., Helgen et al. 2013; Miranda et al. 2018; Machado and Teta 2020).

The results presented here are consistent with findings from previous authors. When D'Orbigny (1834) assigned a full species status to *I. g. boliviensis* (*I. boliviensis*), he did so partly based on the higher number of teeth in their jaws than in *I. geoffrensis*. Van Bree and Robineau (1973) and Silva (1994) also observed similar differences in teeth counts of *I. g. boliviensis*. Furthermore, Ruiz-García et al. (2006) have also shown that *I. g. boliviensis* have a longer rostrum than other groups. Both an increase in teeth count and the length of the rostrum could be associated with differences in diet or predatory behavior (Sydney et al. 2012; McCurry et al. 2017; Page and Cooper 2017; Galatius et al. 2020).
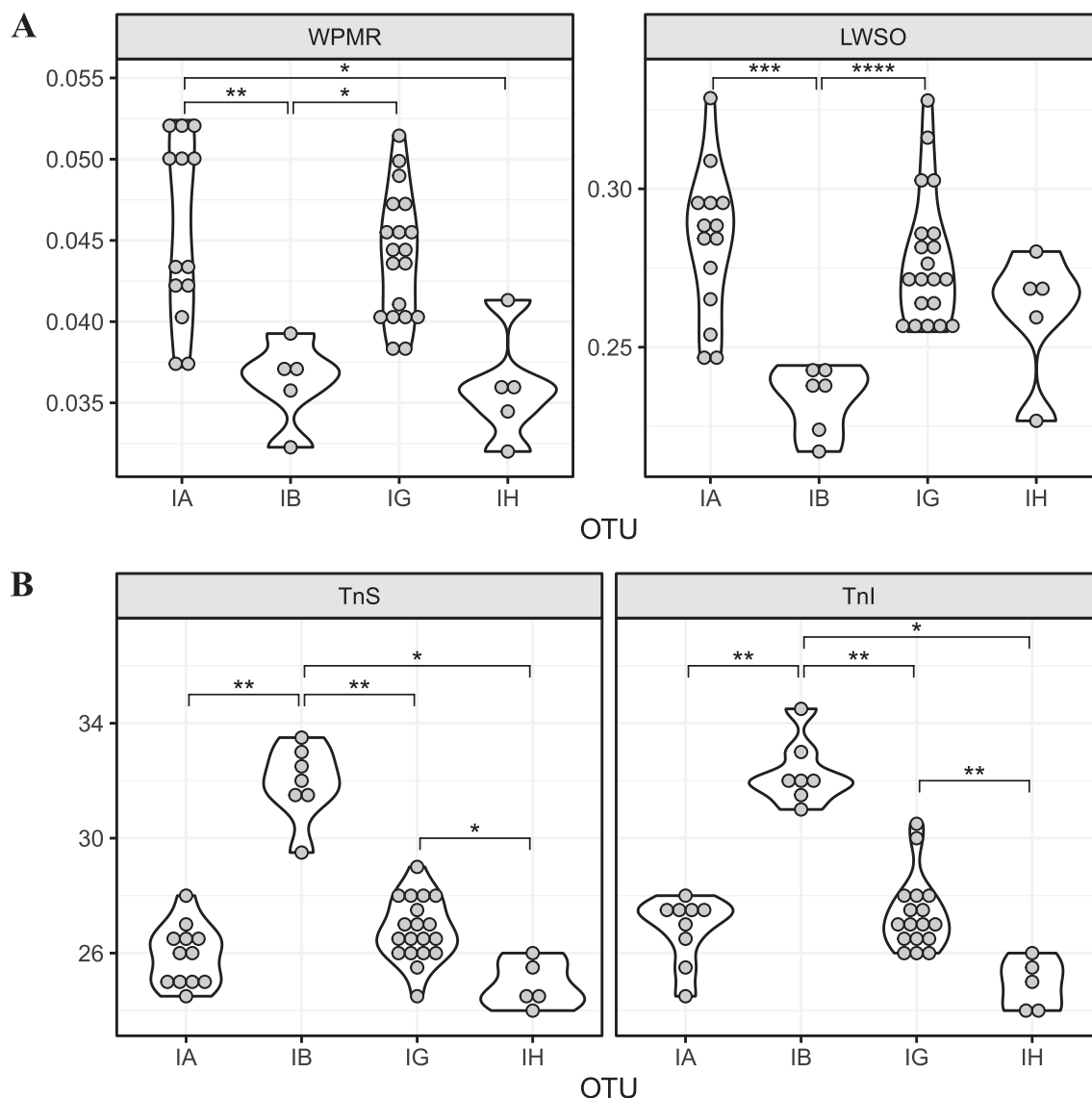
Fig. 6.—Distribution of selected linear distances (A) and teeth count (B) among *Inia* operational taxonomic units (OTUs). (A) Width of premaxillae at midlength of rostrum (WPMR) and least width of supraorbital (LWSO) as a ratio of CBL. (B) Counts of maxillary (TnS) and mandibular (TnI) teeth for different OTUs. Asterisks represent the significance level of the pairwise *t*-tests (A) or Wilcoxon rank-sum tests (B) corrected for multiple comparisons (*$P < 0.05$; **$P < 0.01$; ***$P < 0.001$; ****$P < 0.0001$). IA: *Inia araguaiaensis*; IB: *Inia boliviensis*; IG: *Inia geoffrensis*; and IH: *Inia humboldtiana*.

Pilleri and Gihr (1977) and Cañizales (2020) described morphometric differences of specimens from the Orinoco River basin (*I. g. humboldtiana*) compared to individuals from the Amazon basin (*I. g. geoffrensis*). Specifically, Cañizales (2020) showed that most skull measurements taken from *I. g. humboldtiana* individuals were smaller than *I. g. geoffrensis*, even though he also found considerable size overlap between groups. This difference could be partly due to small sample sizes for *I. g. humboldtiana*—both here and on Cañizales—or a more stringent criterion for adult classification in our study. Regardless, both works agreed that *I. g. humboldtiana* tends to show smaller skulls on average. Similar differences to those described above were also echoed in the external morphology of these groups. Ruiz-García et al. (2006) showed that Amazon basin individuals (*I. g. geoffrensis*)

tend to be larger than both Orinoco basin (*I. g. humboldtiana*) and Bolivian individuals (*I. g. boliviensis*). Together, our analysis and previous reports strongly suggested that the morphological differentiation of *I. g. boliviensis* and *I. g. humboldtiana* were consistent with a specific status for these taxa, a conclusion also suggested by molecular findings (Gravena et al. 2014; Hrbek et al. 2014; Siciliano et al. 2016).

Because we pooled the sexes in our analyses, one could argue that some of the patterns described here are due to sexual dimorphism and sampling bias. Silva (1994) has asserted that *Inia* is a sexually dimorphic group, with males being larger than females, presenting traits that could be up to 15% larger. This could be a problem for the discrimination of *I. g. humboldtiana*, given that this is the only taxon that is different in size alone. However, we were only able to sample males and indeterminate

individuals for these taxa (Table 1). If Silva's (1994) conclusions are valid for all *Inia* groups, then the differences observed for *I. g. humboldtiana* here could be underestimated instead of overestimated. Furthermore, we were unable to identify the presence of a significant sexual dimorphism in our sample of *I. g. geoffrensis*, suggesting further that if *Inia* is indeed sexually dimorphic, the magnitude of dimorphism in the skull is only identifiable in larger sample sizes. Thus, while we acknowledge that more investigations into sexual dimorphism are necessary, we are confident that our results here are not a consequence of sampling bias but rather the reflection of true between-group differences.

The differentiation between *I. araguaiaensis* from *I. g. geoffrensis* is a major topic of debate for *Inia* taxonomy. Previous work had shown that both taxa were genetically distinct and might have been separated from each other for up to 2 Ma (Hrbek et al. 2014; Siciliano et al. 2016). Despite this, we could not differentiate *I. araguaiaensis* from *I. g. geoffrensis* based on their skull morphometrics (Fig. 3–5; Table 3). Our CVA suggests that some *I. araguaiaensis* specimens differ from *I. g. geoffrensis* (Fig. 5), but there is no clear geographical patterning that could explain this disparity, as these outlier specimens can be found both at the delta of the Amazon and along the Araguaia River (Figs. 1 and 5; Appendix I). Therefore, it is not clear if morphometric differentiation attributed to these specimens is representative of species differentiation. However, our failure to identify any significant difference between groups does not necessarily mean that *I. araguaiaensis* and *I. g. geoffrensis* are the same species. For mammals, it is not uncommon to find no, or little morphometric differentiation between reproductively isolated species (e.g., Velazco et al. 2010; Prevosti et al. 2013; Garbino 2015; Feijo et al. 2018; Miranda et al. 2018; Gray et al. 2021; Teta and Reyes-Amaya 2021). The reasons for this can be many, ranging from morphological conservatism due to common ecological pressures (Machado and Teta 2020), confounding effects due to allometric scaling (Prevosti et al. 2013; Machado and Teta 2020), or the lack of representativity of morphometric characters (Salazar-Ciudad and Marín-Riera 2013). Considering that natural selection operates on the overall function of morphological structures rather than the precise shape of smaller components (Salazar-Ciudad and Marín-Riera 2013), it is not unreasonable to assume that two different species would possess very similar overall skull shape as measured through our landmark analysis. A similar process can be observed for *I. g. humboldtiana*—even though our study showed only size-associated differences from *I. g. geoffrensis*, Cañizales (2020) also pointed out the existence of many discrete traits that differentiate these taxa. Thus, it is possible that, despite the lack of morphometric differentiation between groups, both taxa could still present differentiation in morphology that is not accessible to low dimensionality morphometric methods.

Despite being currently recognized as a monotypic genus, we have shown that the morphometric diversity within the genus *Inia* was inconsistent with the single taxon hypothesis. Specifically, we show that specimens from the Orinoco (*I. g. humboldtiana*) and the Beni-Mamoré river basins (*I. g. boliviensis*) were significantly distinct from the remaining populations by size and shape, respectively. While we lacked evidence to show a significant differentiation of the Tocantins–Araguaia basin population (*I. araguaiaensis*) from the Amazon basin group (*I. g. geoffrensis*), genetic analyses have consistently shown that these are disjunct populations with sufficient differentiation to justify the specific status of the former group. Given the conservation importance of these putative species, we call for an urgent integrative taxonomic treatment of the group to better protect these rare cetaceans.

Literature Cited

Adams D.C., Collyer M.L., Kaliontzopoulou A. 2020. Geomorph: software for geometric morphometric analyses. https://cran.r-project.org/package=geomorph. Accessed 22 February 2022.

Aliaga-Rossel E. 2002. Distribution and abundance of the river dolphin (*Inia geoffrensis*) in the Tijamuchi River, Beni, Bolivia. Aquatic Mammals 28:312–323.

Aliaga-Rossel E., Duran L.A.G. 2020. Four decades of research on distribution and abundance of the Bolivian river dolphin *Inia geoffrensis boliviensis*. Endangered Species Research 42:151–165.

Anderson M. 2001. A new method for non-parametric multivariate analysis of variance. Austral Ecology 26:32–46.

Banguera-Hinestroza E., Cárdenas H., Ruiz-García M., Marmontel M., Gaitán E., Vázquez R., García-Vallejo F. 2002. Molecular identification of evolutionarily significant units in the Amazon River dolphin *Inia* sp. (Cetacea: Iniidae). Journal of Heredity 93:312–322.

Best R.C., Silva V.M.F. 1989. Amazon river dolphin, boto, *Inia geoffrensis* (de Blaiville, 1817). In: Ridgway S.H., Harrison R.J., editors. Handbook of marine mammals. Academic Press, London, United Kingdom; p. 23–34.

Braulik G.T., Smith B.D. 2019. *Platanista gangetica*. In: IUCN 2019. The IUCN Red List of Threatened Species. Amended version of 2017 assessment. https://www.iucnredlist.org/species/41758/151913336. Accessed 22 February 2022.

Caballero S., et al. 2007. Taxonomic status of the genus *Sotalia*: species level ranking for "tucuxi" (*Sotalia fluviatilis*) and "costero" (*Sotalia guianensis*) dolphins. Marine Mammal Science 23:358–386.

Cañizales I. 2020. Morphology of the skull of *Inia geoffrensis humboldtiana* Pilleri & Gihr, 1977 (Cetacea: Iniidae): a morphometric and taxonomic analysis. Graellsia 76:1151–1122.

Casinos A., Ocaña J. 1979. A craniometrical study of the genus *Inia* D'Orbigny, 1834, Cetacea, Platanistoidea. Saugetierkunde Mitteilung 27:194–206.

Collyer M.L., Adams D.C. 2018. RRPP: an r package for fitting linear models to high-dimensional data using residual randomization. Methods in Ecology and Evolution 9:1772–1779.

D'Orbigny M. 1834. Notice sur un nouveau genre de cetacé des rivieres du centre de l'Amerique meridionale. Nouveau Annales du Musee d'Historie Naturel de Paris 3:28–36.

Feijo A., Patterson B.D., Cordeiro-Estrela P. 2018. Taxonomic revision of the long-nosed armadillos, genus *Dasypus* Linnaeus, 1758 (Mammalia, Cingulata). PLoS One 13:e0195084.

Fettuccia D.C., Silva V.M.F., Simões-Lopes P.C. 2009. Non-metric characters in two species of *Sotalia* (Gray, 1866) (Cetacea, Delphinidae). Brazilian Journal of Biology 69:907–917.

Galatius A. 2010. Paedomorphosis in two small species of toothed whales (Odontoceti): how and why? Biological Journal of the Linnean Society 99:278–295.

Galatius A., Racicot R., McGowen M., Olsen M.T. 2020. Evolution and diversification of delphinid skull shapes. iScience 23:101543.

Garbino G.S.T. 2015. How many marmoset (Primates: Cebidae: Callitrichinae) genera are there? A phylogenetic analysis based on multiple morphological systems. Cladistics 31:652–678.

Gravena W., Farias I.P., Silva M.N.F., Silva V.M.F., Hrbek T. 2014. Looking to the past and the future: were the Madeira River rapids a geographical barrier to the boto (Cetacea: Iniidae)? Conservation Genetics 15:619–629.

Gravena W., Silva V.M.F., Silva M.N.F., Farias I.P., Hrbek T. 2015. Living between rapids: genetic structure and hybridization in botos (Cetacea: Iniidae: *Inia* spp.) of the Madeira River, Brazil. Biological Journal of the Linnean Society 114:764–777.

Gray H., van Waerebeek K., Owen J., Collins T., Minton G., Ponnampalam L., Willson A., Baldwin R., Hoelzel A.R. 2021. Evolutionary drivers of morphological differentiation among three bottlenose dolphin lineages, *Tursiops* spp. (Delphinidae), in the northwest Indian Ocean utilizing linear and geometric morphometric techniques. Biological Journal of the Linnean Society 135:610–629.

Hamilton H., Caballero S., Collins A.G., Brownell R.L., Jr. 2001. Evolution of river dolphins. Proceedings of the Royal Society of London, Series B: Biological Sciences 268:549–556.

Helgen K.M., Pinto C.C., Kays R., Helgen L.E., Tsuchiya M.T.N., Quinn A., Wilson D.E., Maldonado J.E. 2013. Taxonomic revision of the olingos (*Bassaricyon*), with description of a new species, the olinguito. ZooKeys 324:1–83.

Hollatz C., Vilaça S.T., Redondo R.A.F., Marmontel M., Baker C.S., Santos F.R. 2011. The Amazon River system as an ecological barrier driving genetic differentiation of the pink dolphin (*Inia geoffrensis*). Biological Journal of the Linnean Society 102:812–827.

Hrbek T., Silva V.M.F., Dutra N., Gravena W., Martin A.R., Farias I.P. 2014. A new species of river dolphin from Brazil or: how little do we know our biodiversity. PLoS One 9:1–12.

Klingenberg C.P. 2016. Size, shape, and form: concepts of allometry in geometric morphometrics. Development Genes and Evolution 226:113–137.

Loy A., Tamburelli A., Carlini R., Slice D.E. 2011. Craniometric variation of some Mediterranean and Atlantic populations of *Stenella coeruleoalba* (Mammalia, Delphinidae): a three-dimensional geometric morphometric analysis. Marine Mammal Science 27:E65–E78.

Machado F.A., Teta P. 2020. Morphometric analysis of skull shape reveals unprecedented diversity of African Canidae. Journal of Mammalogy 101:349–360.

McCurry M.R., Fitzgerald E.M.G., Evans A.R., Adams J.W., McHenry C.R. 2017. Skull shape reflects prey size niche in toothed whales. Biological Journal of the Linnean Society 121:936–946.

Meade R., Koehnken L. 1991. Distribution of the river dolphin, tonina *Inia geofrensis* in the Orinoco River Basin of Venezuela and Colombia. Interciencia 16:300–312.

Miranda F.R., Casali D.M., Perini F.A., Machado F.A., Santos F.R. 2018. Taxonomic review of the genus *Cyclopes* Gray, 1821 (Xenarthra: Pilosa), with the revalidation and description of new species. Zoological Journal of the Linnean Society 183:687–721.

Mitteroecker P., Bookstein F.L. 2011. Linear discrimination, ordination, and the visualization of selection gradients in modern morphometrics. Evolutionary Biology 38:100–114.

Mitteroecker P., Gunz P., Bernhard M., Schaefer K., Bookstein F.L. 2004. Comparison of cranial ontogenetic trajectories among great apes and humans. Journal of Human Evolution 46:679–697.

Monteiro-Filho, E.L.D.A., Monteiro L.R., Reis S.F.D. 2002. Skull shape and size divergence in dolphins of the genus *Sotalia*: a tridimensional morphometric analysis. Journal of Mammalogy 83:125–134.

Oliveira L.R., Hingst-Zaher E H.J., Majluf P., Muelbert M., Morgante J.S., Amos W. 2008. Morphological and genetic evidence for two evolutionarily significant units (ESUS) in the South American fur seal, *Arctocephalus australis*. Conservation Genetics 9:1451–1466.

Page C.E., Cooper N. 2017. Morphological convergence in "river dolphin" skulls. PeerJ 5:e4090.

Perrin W.F. 1975. Variation of spotted and spinner porpoises (genus *Stenella*) in the Eastern Pacific and Hawaii. Bulletin of the Scripps Institution of Oceanography 21:1–206.

Pilleri G., Gihr M. 1977. Observations on the Bolivian, *Inia boliviensis*, (D'Orbigny, 1834) and the Amazonian bufeo, *Inia geoffrensis* (Blainville, 1817), with a description of a new subspecies (*Inia geoffrensis humboldtiana*). In: Pilleri G., editor. Investigations on Cetacea. Institute of Brain Anatomy/University of Berne, Bogotá, Colombia; p. 11–76.

Prevosti F.J., Segura V., Cassini G., Martin G.M. 2013. Revision of the systematic status of patagonian and pampean gray foxes (Canidae: *Lycalopex griseus* and *L. gymnocercus*) using 3D geometric morphometrics. Mastozoología Neotropical 20:289–300.

R Core Team. 2021. R: a language and environment for statistical computing. R Foundation for Statistical Computing, Vienna, Austria. https://www.r-project.org/. Accessed 23 February 2022.

Rice, D.W. 1998. Marine mammals of the world. Systematics and distribution. Special Publication No. 4. The Society for Marine Mammalogy, Allen Press Inc., Lawrence, Kansas. v-ix+231pp.

Rohlf F.J., Slice D.E. 1990. Extensions of the Procrustes method for the optimal superimposition of landmarks. Systematic Zoology 39:40–59.

Ruiz-García M., Banguera E., Cardenas H. 2006. Morphological analysis of three *Inia* (Cetacea: Iniidae) populations from Colombia and Bolivia. Acta Theriologica 51:411–426.

Salazar-Ciudad I., Marín-Riera M. 2013. Adaptive dynamics under development-based genotype-phenotype maps. Nature 497:361–364.

Siciliano S., Valiati V.H., Emin-Lima R., Costa A.F., Sartor J., Dorneles T., Sousa e Silva J., Jr., Oliveira L.R. 2016. New genetic data extend the range of river dolphins *Inia* in the Amazon Delta. Hydrobiologia 777:255–269.

Silva V., Trujillo F., Martin A., Zerbini A.N., Crespo E., Aliaga-Rossel E., Reeves R. 2018. *Inia geoffrensis*. In: IUCN 2018. The IUCN Red List of Threatened Species. Version 2018. e.T10831A50358152. https://dx.doi.org/10.2305/IUCN.UK.2018-2.RLTS.T10831A50358152.en. Accessed 23 February 2022.

Silva, V.M.F. 1994. Aspects of the biology of the Amazonian dolphins genus *Inia* and *Sotalia fluviatilis*. Ph.D. thesis, The University of Cambridge, Cambridge, United Kingdom. 327 p.

Slice D. 2001. Landmark coordinates aligned by procrustes analysis do not lie in Kendall's shape space. Systematic Biology 50:141–149.

Smith B.D., Wang D., Braulik G.T., Reeves R., Zhou K., Barlow J., Pitman R.L. 2017. *Lipotes vexillifer*. In: IUCN 2017. The IUCN Red List of Threatened Species. Version 2017. e.T12119A50362206. https://dx.doi.org/10.2305/IUCN.UK.2017-3.RLTS.T12119A50362206.en. Accessed 23 February 2022.

Society for Marine Mammalogy Committee on Taxonomy [SMMCT]. 2021. List of marine mammal species and subspecies. Committee on Taxonomy. www.marinemammalscience.org. Accessed 23 February 2022.

Strauss R. 2010. Discriminating groups of organisms. In: Elewa A.M.T, editor. Morphometrics for nonmorphometricians. Springer, Berlin; p. 73–91.

Sydney N.V., Machado F.A., Hingst-Zaher E. 2012. Timing of ontogenetic changes of two cranial regions in *Sotalia guianensis* (Delphinidae). Mammalian Biology - Zeitschrift fur Saugetierkunde 77:397–403.

Teta P., Reyes-Amaya N. 2021. Uncovering species boundaries through qualitative and quantitative morphology in the genus *Dasyprocta* (Rodentia, Caviomorpha), with emphasis in *D. punctata* and *D. variegata*. Journal of Mammalogy 102:1548–1563.

Van Bree P.J.H., Robineau D. 1973. Notes sur les holotype de *Inia geoffrensis* (de Blainville, 1817) et de *Inia boliviensis* (D'Orbigny, 1834) (Cetacea, Platanistidae). Mammalia 37:558–664.

Velazco P.M., Gardner A.L., Patterson B.D. 2010. Systematics of the *Platyrrhinus helleri* species complex (Chiroptera: Phyllostomidae), with descriptions of two new species. Zoological Journal of the Linnean Society 159:785–812.

Wickert J.C., Von Eye S.M., Oliveira L.R., Moreno I.B. 2016. Revalidation of *Tursiops gephyreus* Lahille, 1908 (Cetartiodactyla: Delphinidae) from the southwestern Atlantic Ocean. Journal of Mammalogy 97:1728–1737.

Zerbini A.N., Secchi E.R., Crespo E.A., Danilewicz D., Reeves R.R. 2018. *Pontoporia blainvillei*. In: IUCN 2017. The IUCN Red List of Threatened Species. Errata version published in 2018. e.T17978A123792204. https://dx.doi.org/10.2305/IUCN.UK.2017-3.RLTS.T17978A50371075.en. Accessed 23 February 2022.

APPENDIX I

Specimens analyzed. ♂—male. ♀—female.

Inia araguaiaensis—**BRAZIL**—*Mato Grosso*: Rio das Mortes—MZUSP 7008♂; *Pará*: Curuçá—MPEG 42122, MPEG 42139, MPEG 42182; Salvaterra—MPEG 38764, MPEG 42044; Soure—MPEG 42055♀, MPEG 42169, MPEG 42170, GEMAM 702; *Tocantins*: Formoso do Araguaia—UFT 24, MCN-M 32♂, MCN-M 89.

Inia geoffrensis geoffrensis—**BRAZIL**—*Amazonas*—MN 6425♀; *Pará*: Altamira—MPEG 12756♂; Bella Imperatriz Vilage, Rio Amazonas—AMNH 93412♂, AMNH 93413♂, AMNH 93414♀, AMNH 93415♀; Inajatuba, Rio Tapajós—AMNH 95753♀; Santarém—MPEG 4608♀, MPEG 4609♂, MPEG 4642♂, MPEG 39626; Rio

Tapajós—MN 6424♂, MN 6423♂, MN 24959; **PERU**—AMNH 98695; *Ucayali*, Rio Tamaya—AMNH 147502, AMNH 147503.

Inia geoffrensis boliviensis—**BOLIVIA**—Bol 01, Bol 02; *Dept. Beni*, Río Baures—AMNH 209105♂; Río Mamoré—AMNH 209101♂; Río Itenéz—AMNH 209103♀, AMNH 209104; Río Mamoré (opposite to Costa Marques) —AMNH 209102♀.

Inia geoffrensis humboldtiana—**VENEZUELA**—USNM 406801; *Apure*—USNM 395415♀, USNM 395416♀, USNM 396166♀.

APPENDIX II

List of landmarks (numbers) and linear measurements (acronyms) taken on the skull and mandible of *Inia*.

1. Anterior point of the right premaxilla.
2. Right suture of premaxilla and maxilla at the 15th alveolus (anteroposterior direction).
3. Left suture of premaxilla and maxilla at the 15th alveolus (anteroposterior direction).
4. Posterior margin of the right anteriormost infraorbital foramen.
5. Posterior margin of the left anteriormost infraorbital foramen.
6. Intersection between the ethmoid and the suture of the nasal bones.
7. Posteriormost point of the right premaxilla.
8. Posteriormost point of the left premaxilla.
9. Anteriormost point of the suture between the frontal and interparietal bones.
10. Right frontal-pariental-occipital suture.
11. Left frontal-pariental-occipital suture.
12. Right posteriormost point of the temporal crest.
13. Left posteriormost point of the temporal crest.
14. Right antorbital notch.
15. Left antorbital notch.
16. Anteriormost point between the right maxilla and lacrimal.
17. Anteriormost point between the left maxilla and lacrimal.
18. Right posteriormost point of the orbital process.
19. Left posteriormost point of the orbital process.
20. Right anteriormost point of the squamosal.
21. Left anteriormost point of the squamosal.
22. Right anteriormost point of lacrimal.
23. Left anteriormost point of lacrimal.
24. Dorsal margin of the foramen magnum.
25. Ventral margin of the foramen magnum.
26. Right internal dorsal margin of the occipital condyle.
27. Left internal dorsal margin of the occipital condyle.
28. Right internal ventral margin of the occipital condyle.
29. Left internal ventral margin of the occipital condyle.

CBL: Condylobasal length
LR: Length of the rostrum
WRB: Width of the rostrum at base
WRM: Width of the rostrum at midlength
WPMR: Width of premaxillae at midlength of the rostrum

LREN: Length of the rostrum to the base of the external nares
GWPE: Greatest width of preorbital
GWPO: Greatest width of postorbital
LWSO: Least width of supraorbital
GWEN: Greatest width of external nasals
GWZS: Greatest width of zygomatic at squamosal
GWP: Greatest width of premaxillae
WP: Width of parietal
GLTFL: Greatest length of the left temporal fossa

GHTFL: Greatest height of left temporal fossa, perpendicular to the greatest length
LLLTR: Length of lower left tooth row
GHLM: Greatest height of the left mandible, using the greatest length
GHFM: Greatest height of foramen magnum
GWFM: Greatest width of the foramen magnum
GHLOC: Greatest height of left occipital condyle
GWLOC: Greatest width of the left occipital condyle